ECOLOGY

Hippos (*Hippopotamus amphibius*): The animal silicon pump

Jonas Schoelynck[1]*, Amanda L. Subalusky[2,3], Eric Struyf[1], Christopher L. Dutton[3], Dácil Unzué-Belmonte[1], Bart Van de Vijver[1,4], David M. Post[3], Emma J. Rosi[2], Patrick Meire[1], Patrick Frings[5,6]

While the importance of grasslands in terrestrial silicon (Si) cycling and fluxes to rivers is established, the influence of large grazers has not been considered. Here, we show that hippopotamuses are key actors in the savannah biogeochemical Si cycle. Through a detailed analysis of Si concentrations and stable isotope compositions in multiple ecosystem compartments of a savannah-river continuum, we constrain the processes influencing the Si flux. Hippos transport 0.4 metric tons of Si day^{-1} by foraging grass on land and directly egesting in the water. As such, they bypass complex retention processes in secondary soil Si pools. By balancing internal processes of dissolution and precipitation in the river sediment, we calculate that hippos affect up to 76% of the total Si flux. This can have a large impact on downstream lake ecosystems, where Si availability directly affects primary production in the diatom-dominated phytoplankton communities.

INTRODUCTION

Animals play an important role in the distribution of resources across landscapes, because of their capacity to ingest large quantities of food in a different location than that in which they egest, excrete, or die (*1*, *2*). This resource translocation has important effects on carbon and nutrient cycling, ecosystem productivity, and food web structure in both the source and recipient ecosystems (*3*, *4*). Studies of animals have predominantly focused on the biogeochemical cycles of the nutrients C, N, and P, but animals also move other elements that are essential to biological processes, such as silicon (Si). Although our understanding of the biogeochemical Si cycle, and the strong biotic control on global Si fluxes, has evolved markedly over the past decades, we have yet to integrate the potential role of large fauna into this cycle.

Scientific understanding of the Si cycle has progressed from conceptualizing it as almost purely driven by geological processes to a much more nuanced understanding that includes biological transformation and cycling. Mineral weathering is the ultimate source of all dissolved Si in rivers and the oceans, but biota in terrestrial ecosystems typically control an important portion of continental Si fluxes (*5*). Studies in various ecosystems demonstrate that vegetation increases the retention time of Si as it moves from the land toward the rivers and ultimately the ocean [see (*6*) for a review]. Plants take up weathered Si from the soil and accumulate it in amorphous biogenic silica particles called phytoliths. When plants die and decompose, a large biogenic Si stock is built up in ecosystem soils, and its persistence, transformation into secondary Si-pools, and stability exert a strong control on continental Si export (*5*).

Quantifying Si export from land to water is crucial for understanding lake and coastal biogeochemistry (*7*). Diatoms (Bacillariophyta), which use biologically available Si from the water to form their frustules, are predominant contributors to global carbon fixation, carrying out about 20% of photosynthesis on Earth (*8*). Si limitation can put a strong constraint on their production (*9*). Multiple studies highlight how the high productivity of the East African lakes depends on river Si inputs, as diatoms form the base of their food webs [e.g., Lakes Victoria and Albert (*10*), Malawi (*11*), Tanganyika (*12*)]. If riverine Si delivery to these lakes is reduced, then this could induce algal community shifts with knock-on effects on the food web structure and human well-being in that region (*13*).

The common hippopotamus (*Hippopotamus amphibius* L. 1758, hereafter "hippo") warrants attention when considering Si mobility in the East African lake area, due to its unique feeding patterns. Hippos are semi-aquatic and have a diel activity pattern: Hippos feed in savannah grasslands at night and typically rest communally in river meanders (hereafter "hippo pools") during the day. Hippos contribute large amounts of C, N, and P to aquatic systems through these grazing, moving, and egesting patterns (*14*). The accompanying, yet unknown, transfer of Si (both in the form of fecal biogenic Si and Si dissolved out of the feces in suspension) could thus bypass the cycling of Si in soils, where reuptake of dissolved Si by plants or precipitation of dissolved Si as authigenic (alumino-)silicate phases greatly slows Si export (*5*). This direct transfer from terrestrial to aquatic ecosystems is analogous to the loss of biogenic Si from soils via crop harvest, inducing soil Si depletion (*15*). In contrast to the large amounts of harvested biogenic Si from crops that are potentially lost to biological cycling on longer time scales and stored in the anthroposphere (*15*), the biogenic Si consumed by hippos may largely be transported directly to the river and may become readily available for downstream primary producers: a land-to-river Si pump driven by animals. To provide evidence for the animal Si pump hypothesis and to quantify its contribution to the overall downstream Si flux, we undertook detailed field sampling in a hippo-dominated ecosystem in south-western Kenya.

RESULTS

Fluxes and mass balance of Si in the Maasai Mara National Reserve

At the time of sampling, daily fluxes of dissolved and biogenic Si through the Mara River in Kenya were 7.9 and 2.4 metric tons, respectively (Fig. 1).

[1]University of Antwerp, Department of Biology, Ecosystem Management Research Group, Universiteitsplein 1C, B-2610 Wilrijk, Belgium. [2]Cary Institute of Ecosystem Studies, Millbrook, NY, USA. [3]Yale University, Department of Ecology and Evolutionary Biology, New Haven, CT, USA. [4]Botanic Garden Meise, Nieuwelaan 38, 1860 Meise, Belgium. [5]Department of Geosciences, Swedish Museum of Natural History, Box 50007, Stockholm, Sweden. [6]Section 3.3 Earth Surface Geochemistry, GFZ German Research Centre for Geosciences, Telegrafenberg, Potsdam, Germany. *Corresponding author. Email: jonas.schoelynck@uantwerp.be

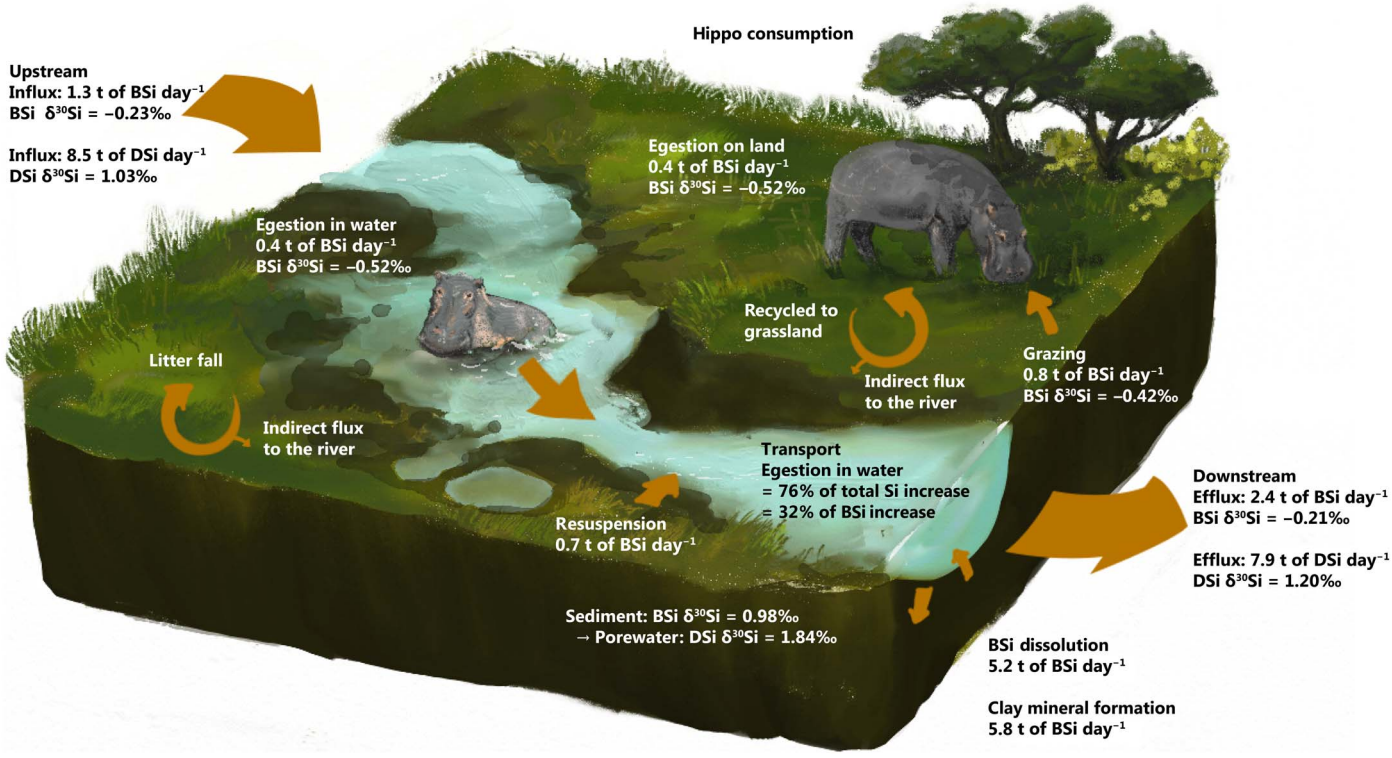

Fig. 1. Conservative Si mass balance of the Mara River. Upstream influx and downstream efflux is calculated by multiplying dissolved Si (DSi) and biogenic Si (BSi) concentrations at sites 1 and 10 (table S1) with a 10-day averaged discharge at both locations, respectively. The lateral influx by hippo egestion is calculated by multiplying the average biogenic Si concentration in feces (table S1) with the conservative estimate of feces deposition in the river [11.1 metric tons of DM day^{-1} (*14*)]. The average biogenic Si concentration in grass (table S1) is multiplied with the conservative estimate of grass eaten [42.0 metric tons of DM day^{-1} (*14*)] to calculate the uptake of biogenic Si by grazing. The difference between uptake and egestion in the water is the egestion on land. The difference between Si flux upstream and downstream is the Si that is added to the water from the MMNR. Biogenic Si dissolution and clay mineral formation are calculated using a Si isotope mass balance model (see the Supplementary Materials). Concentrations are reported as mass of Si. t, metric tons.

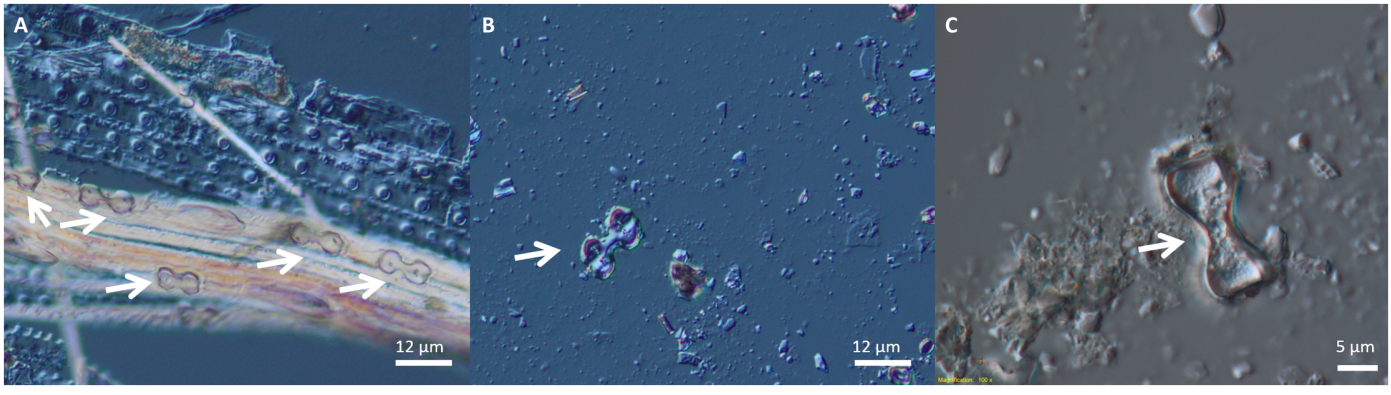

Fig. 2. Dumbbell-shaped phytoliths (indicated with white arrows). These phytoliths were found in grass (**A**), hippo feces (**B**), and suspended matter and sediment (**C**). Phytoliths account for 98 to 99% of total biogenic Si particle counts in suspended matter and sediment samples (see also fig. S1 for more and different pictures).

Along the sampling gradient, biogenic Si flux gradually increased. In situ biogenic Si production by diatoms can be excluded as a cause, as very few diatom frustules or chrysophyte stomatocysts (1 to 2% of total biogenic Si particle count) were found in suspended matter and sediment samples (Fig. 2 and fig. S1), contrary to observations made in, e.g., the Congo River (*16*). Biogenic Si in the Mara River suspended matter and sediment samples consisted almost entirely of phytoliths or phytolith remains, confirming its terrestrial origin (*17*). Maasai Mara National Reserve (MMNR) grass biogenic Si concentrations were, on average, 1.8% of plant dry weight (table S1), and biogenic Si concentrations were further elevated in hippo feces (on average, 4.1% of feces dry weight; table S1). Increasing concentration in temperate domestic grazer feces was related to the digestion of organic matter in the digestive tract, consequently increasing biogenic Si concentrations (*18*). The flux of grass

biogenic Si through the hippos toward the river during the dry season is large: The daily loading directly into the river by excretion and egestion of the hippo population in the MMNR equals 11.1 metric tons of DM of feces (*14*), which renders a flux of 0.4 metric tons of biogenic Si day^{-1} into the river. A dissolved Si flux through urine was not measured but is approximately 3% of the total grazed Si in other herbivore species (*18*).

Continuous monitoring of Si and Al concentrations during laboratory alkaline extractions, an analytical method to distinguish between biogenic and nonbiogenic Si (see Material and Methods for more details and background information), confirms that, essentially, all of the alkaline reactive Si in suspended matter is of biological origin (table S1). A small (up to 0.8%) alkaline-extractable fraction of nonbiological origin (found at sites 1, 4, 8, and 10) likely originates from erosion of the savannah soil, where similar fractions are found (table S1).

This estimated direct biogenic Si influx to the river through hippos accounts for 32% of the increase in biogenic Si flux from the most upstream sample site to the most downstream site (Fig. 1). The remaining 68% is likely attributed to resuspension of bed material (*19*) containing older feces, alternative inputs (e.g., dust), and indirect inputs (e.g., hippo and other animal feces on the banks close to the river). These estimates are corroborated by the high-resolution monitoring of a hippo pool over a 24-hour period: Over a 250-m stretch with up to 80 hippos present, river biogenic Si concentrations doubled relative to upstream values (Fig. 3). This was solely attributed to fresh egestion by the animals and stirring up of bed and bank material.

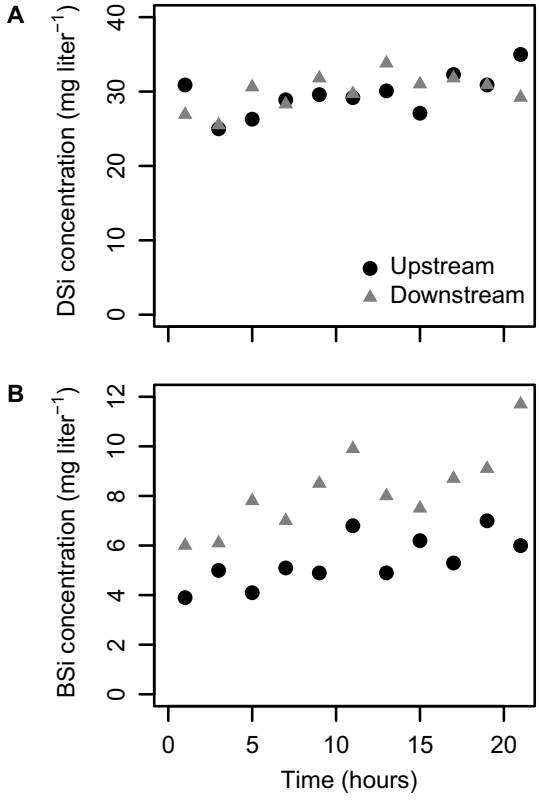

Fig. 3. Changes in silicon concentrations after river water has passed through a hippo pool. Duration, 24 hours; length of reach, 250 m; up to 80 hippos were present. (**A**) Dissolved Si concentrations. (**B**) Biogenic Si concentrations. All concentrations are reported as mass of Si.

After 24-hour dissolution in rain water, 2.8% of fresh hippo feces biogenic Si was dissolved, which is 17.2 times more than that of undigested grass in similar conditions, yet it decreases with the age of the feces (Fig. 4). This influence of digestion agrees with similar experiments on the feces of domesticated grazers (*18*). The enhancement of dissolution by the pseudoruminant hippo is higher than that of the ruminant cow (*Bos primigenius taurus*; 2.0 times faster than undigested hay) and the hindgut fermenter horse (*Equus ferus caballus*; 1.2 times faster than undigested hay), highlighting the importance of food source and digestion style on Si solubility (*18*).

Isotopic constraints on MMNR Si cycling

The total dissolved Si flux decreased by ca. 7% toward the end of the sampling gradient (Fig. 1 and table S1), suggesting a slight net retention of dissolved Si within the Mara River. Si isotope values (expressed as δ^{30}Si) of river dissolved Si fluctuate by 0.7 per mil (‰), with a slight net increase of approximately 0.17‰ over the entire study reach (Fig. 5) and correlate positively with dissolved Si fluxes at progressively downstream sampling points (fig. S2, A and B). Although not fully mechanistically understood, previous work allows generalizations about Si isotope fractionation to be drawn. First, the removal of Si from a dissolved pool almost always discriminates against the heavier isotopes of Si, leaving the residual solution enriched in ^{30}Si (higher δ^{30}Si). Second, the addition of Si to a dissolved pool also almost always favors the lighter isotopes because all potential solid sources have lower δ^{30}Si values.

The Si isotope behavior in the Mara is not readily consistent with these principles. The small decrease in dissolved Si flux does occur together with an increase in δ^{30}Si over the entire length of the river, but estimates of Si isotope fractionations associated with biogenic uptake or authigenic clay formation [reviewed in (*20*)] are mostly too small to produce a net δ^{30}Si increase of ca. 0.2‰ for a removal of only 7%. More problematically, δ^{30}Si and dissolved Si fluxes over the length of the river are positively correlated (fig. S2, A and B). This relationship is counter to observations from other river studies (*20*) and opposite in direction to that predicted from any known fractionation. On short time scales, this pattern can be explained by the mixing of high-δ^{30}Si riparian zone porewaters with Mara River water, but these porewaters constitute a finite pool of Si. The challenge is thus to explain how high [Si] and high-δ^{30}Si riparian zone porewaters are generated.

Biological Si uptake, secondary abiotic Si precipitation, and dissolved Si release through weathering all discriminate against the heavier Si isotopes. The proximate explanation for the increase in δ^{30}Si of river dissolved Si is the admixture of high-δ^{30}Si riparian porewater, but the ultimate explanation must involve processes that remove Si from solution. To quantify Si processing in more detail in the MMNR, we constructed a mass balance of the system, constrained by the isotopic signatures (see details in the Supplementary Materials). Together with a Monte Carlo approach to propagate the uncertainties, this analysis suggests that two processes acting in unison can explain the observations: One removes Si from solution, while the second adds Si at approximately the same rate, with the slight rate imbalance resulting in the small decrease in net dissolved Si flux. Schematically, we refer to these processes as "clay mineral formation" and "biogenic Si dissolution," respectively (Fig. 1), although we recognize that a suite of other processes could be contributing. The mass balance predicts that, cumulatively, over the course of the entire study reach, ca. 5.2 metric tons of Si day^{-1} is solubilized from phytoliths in the channel or riparian zone. The feasibility of this value is corroborated by the dung dissolution

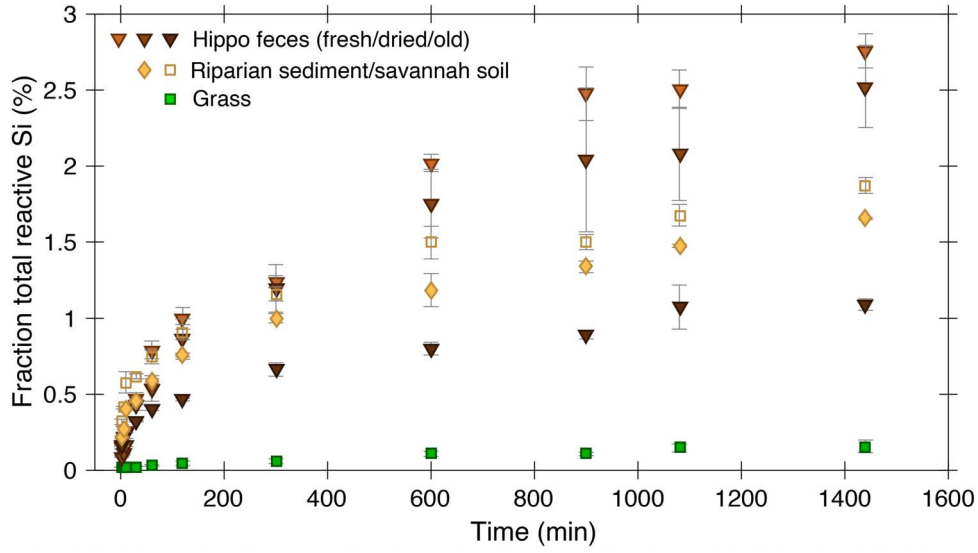

Fig. 4. Dissolution of reactive Si in samples of different river compartments after exposure to rain water during 24 hours (1440 min). Results are expressed as percentage (%) of the total reactive Si (reported as mass of Si) in the samples [biogenic Si in grass and feces and alkaline-extractable Si (AlkExSi) determined with the continuous analysis method (*42*) for other samples] and are plotted as mean values (symbols) with SDs (error bars; $n = 5$). Series are fresh feces (order of hours old), dried feces (order of days old), old feces (order of weeks old), grass, sediment, and savannah soil.

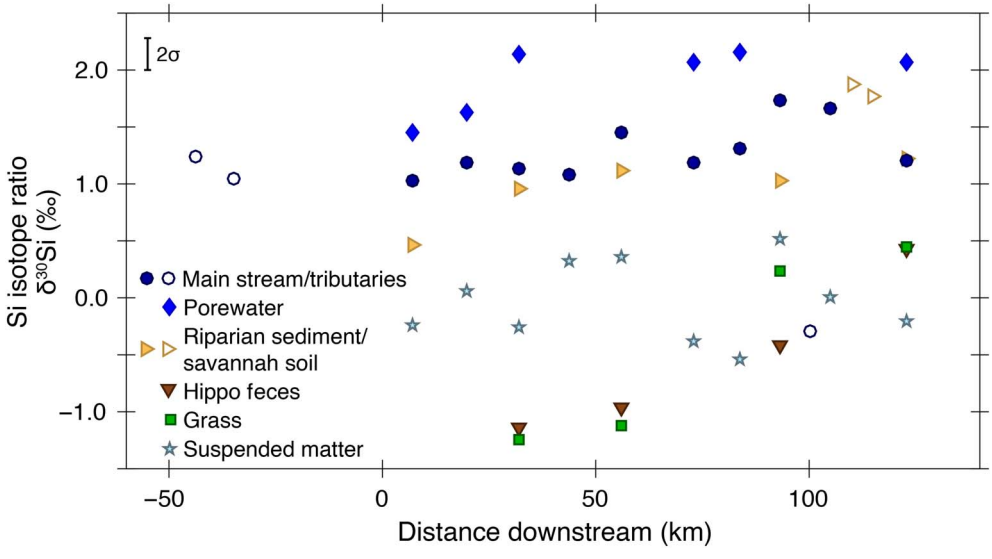

Fig. 5. δ^{30}Si values (in ‰ relative to the NBS28 quartz sand standard) of different ecosystem compartments. Each compartment of the terrestrial-aquatic Si supply chain had a relatively narrow range of δ^{30}Si values. Mean values (±1σ) in grass (−0.42 ± 0.89‰), hippo feces (−0.52 ± 0.71‰), and suspended matter (−0.04 ± 0.35‰) are in close agreement with each other, although suspended matter is somewhat higher. δ^{30}Si values in sediment (0.93 ± 0.43‰), river water dissolved Si (1.30 ± 0.24‰), savannah soil (1.83 ± 0.08), and porewater dissolved Si (1.84 ± 0.33‰) are higher, with savannah soil and porewater clearly distinct from river water and sediment.

experiments (Fig. 4 and fig. S3) and river biogenic Si measurements (see the Supplementary Materials). Crucially, this value is only attainable using the experimental phytolith dissolution rates of hippo feces—undigested material does not dissolve rapidly enough (fig. S3A). Conversely, 5.8 metric tons of Si day^{-1} is precipitated into secondary clays with the model predicting a reasonable range of associated fractionations. Thus, a difference of 0.6 metric tons of Si day^{-1} is lost from the system as clay minerals. This balance provides a smart and internally consistent explanation for the high δ^{30}Si and high [Si] in porewaters and the positive covariation between dissolved Si flux and δ^{30}Si of the dissolved Si.

One key term in the Si isotope mass balance is the δ^{30}Si of the dissolving biogenic Si and any fractionation that might be associated with its dissolution (see the Supplementary Materials). Grass had the lowest δ^{30}Si in the MMNR: Plants discriminate against ^{30}Si during Si uptake (*21*). The amount of Si retained in an animal after ingestion of plants is negligible (*22*), and this is reflected in the near-identical δ^{30}Si of grass and feces. Grass δ^{30}Si values are variable along the river transect (and likely spatially at each sampling site), which could be related to variable plant rooting depth (i.e., dissolved Si source), plant age, and grazing intensity (affecting the age of sampled material). The exact mechanisms driving plant δ^{30}Si heterogeneity are beyond the scope

of this study, although the pattern warrants future investigation. River suspended biogenic Si generally has higher δ^{30}Si than the grass or feces from which it derives, and it is less variable over the whole river stretch. A kinetic fractionation should favor the transfer of lighter isotopes to solution (*23*, *24*), so incomplete dissolution of feces with an associated isotope fractionation may leave the residual biogenic Si enriched in ^{30}Si and thus explain the higher suspended sediment biogenic Si δ^{30}Si values. It is clear from the dissolution kinetics that the rate of Si dissolving from feces in water decreases with the age of the feces (Fig. 4). δ^{30}Si value of feces also increases with age: Fresh feces (−0.52‰) has a lighter signature than old feces (+0.20‰), corroborating the existence of a fractionation during dung dissolution, although the implicit assumption of a common initial value is difficult to verify.

Sedimentary biogenic Si δ^{30}Si values are considerably higher than the suspended matter it derives from and generally decrease with depth. This sediment is likely a mixture of relatively slowly dissolving aged feces with δ^{30}Si values higher than fresh feces and relatively quickly dissolving savannah soil particles (Fig. 4) with higher δ^{30}Si. A mixture of material with different dissolution kinetics and different δ^{30}Si values can explain the generally high δ^{30}Si values in the sediment.

The formation of secondary mineral phases in the sediment, in turn, can explain the high porewater δ^{30}Si. In general, secondary phase formation is characterized by a fractionation that leaves the heavier isotopes in the residual solution (*25*). Our mass balance (see the Supplementary Materials) requires isotope fractionations of between −2.8 and −1.5‰, in good agreement with observations. Other processes might also contribute to the high porewater δ^{30}Si values. Dissolution of savannah soil particles in the sediment (with similarly high δ^{30}Si values as in porewater; Fig. 5) may push porewater values even higher.

DISCUSSION

Hippos are an animal Si pump

We conclude that hippos play a key role in Si cycling as a terrestrial-aquatic pump, contributing 32% to the biogenic Si flux and more than 76% to the total Si flux along the Mara River. These values come from conservative estimations of Si stocks and fluxes between all relevant ecosystem compartments, based on dry season estimates and measurements. Our estimates for hippo loading into the river suggest that hippos are likely to consume and egest less organic matter in the wet season, due to the higher nutritional content of plants during this season and subsequent lower consumption rate, although this lower input to the river may be offset by increased time spent in the river because of more abundant forage (*14*). River discharge and background Si flux also are likely to increase in the wet season, which may increase Si transport; however, the dilution effect may lead to either increased or decreased Si fluxes. Together, these seasonal factors suggest that the dry season estimates presented here may be on the upper end of the proportion of Si cycling mediated by hippos. However, other research has shown that our annual estimates of hippo loading into the Mara River, based on an average of wet and dry season values, compare fairly well with our measurements of C and nutrient fluxes in the river and that high levels of loading in the dry season are often stored in the channel and are transported downstream in the wet season (*26*), suggesting that the estimates presented here are reasonable approximations of hippo influence on Si flux.

Our modeling approach also required balancing out internal processes of dissolution and precipitation in the river sediment. This Si cycling balance requires the assumption of an "infinitely" large sediment biogenic Si stock from which (i) biogenic Si may resuspend and (ii) phytoliths may dissolve and precipitate into clays. Notwithstanding, the sediment layer can be quite thick (personal observation); a more likely explanation is that sedimentation and resuspension dynamics are spatially and seasonally (and even day to day) strongly variable and depend on fluctuations in flow velocity in the river. During periods of slow flow and low turbulence, hippos likely oversaturate the river with feces, and the sediment biogenic Si stock is replenished. During periods of fast flow and high turbulence, biogenic Si gets resuspended. A similar impact of phytoliths on internal Si cycling was found in the Okavango Delta, a subtropical flood-pulse wetland in Northern Botswana (*27*). However, it is unprecedented in rivers, which highlights the key role of the hippo as a land-to-river Si pump in the ecosystem.

The role of other grazers

The role of other grazers in the savannah ecosystem was only marginally touched upon in this study. Feces from other animals that are egested while the animals drink from the water source will likely add additional Si to the river, which could partly explain the discrepancy between calculated hippo inputs and the measured increase in biogenic Si from upstream to downstream, together with sediment resuspension and dust. Moreover, some species have a larger food intake and/or larger day ranges (e.g., elephants), while other species are far more numerous than the hippo (e.g., antelope species), which makes them potentially important Si pumps as well. Although the role of these herbivores in making nutrients (and Si) available in the landscape is incontestable (*28*), hippos are unique in their diel grazing and egestion rhythm (see Introduction). For non-hippo grazers, it is difficult to estimate how much Si can reach the river rather than be recycled on land (*5*). Research on the effects of sheep grazing on Wadden Sea saltmarshes (Germany) showed that export rates from grazed sites were actually lower than those from ungrazed sites, although this result was explained by grazer-induced changes to local hydrology and differences in benthic diatom uptake (*29*). The differing characteristics and responses of the two ecosystems limit their comparability and underscore the need to consider each system holistically.

How would the Mara ecosystem look without hippos?

Unintended downstream repercussions to Lake Victoria and other Rift Valley lake ecology are possible if hippos are removed from the savannah ecosystem. A substantial part of the Si in the Mara River is transported downstream into Tanzania and potentially further into Lake Victoria. Most rivers draining into Lake Victoria, however, have been cleared of hippo populations, which are currently confined to the mouths of major rivers and littoral areas around the lake (*30*). Throughout Africa, hippo populations have decreased by 7 to 20% from 1996 to 2004 and are expected to decrease by a further 30% over the next three generations following global defaunation trends (*31*).

If all hippos in the Mara River disappeared and the direct input of biogenic Si ceased, then we would expect an immediate reduction in total Si transport. This reduction might be relatively greater in catchments where the underlying bedrock results in lower baseline Si concentrations than the volcanic lithology of the Mara River basin. This reduction could be sufficient to further limit diatom growth in Lake Victoria, where increased N:Si and P:Si ratios have already caused a phytoplankton transition to year-round dominance by cyanobacteria since the late 1980s (*32*), and the diversity of planktonic diatom communities has declined markedly (*33*). Diatoms need an optimal nutrient

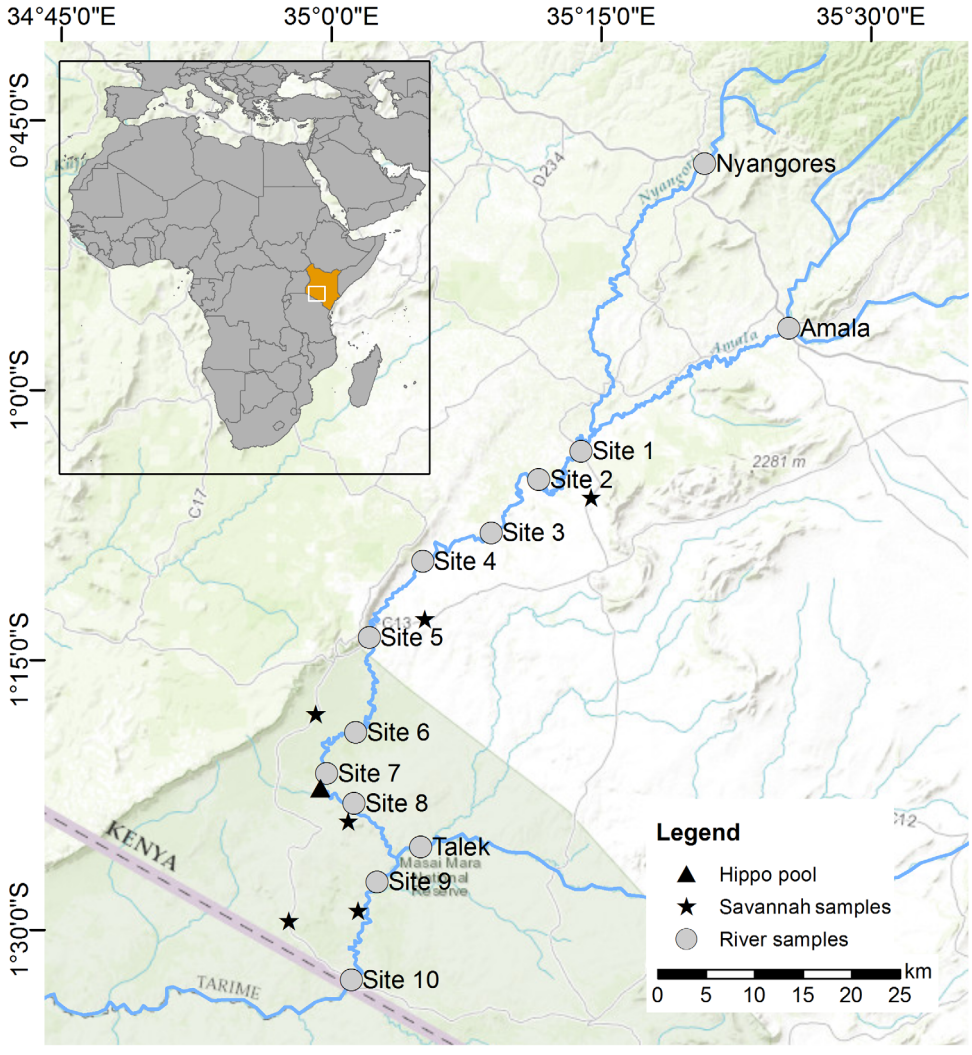

Fig. 6. Map of the field sites in the MMNR (Kenya).

ratio of C:Si:N:P (106:15:16:1), and diatom growth will cease when Si supplies are depleted, allowing other phytoplankton classes to proliferate using any excess N and P (*34*). Similar transitions have been documented for other Rift Valley lakes, where climate change and human use of N and P in the watershed increased N:Si and P:Si ratios [e.g., Lake Tanganyika (*35*)]. However, a decreased Si flux to the lakes could also be part of the problem. Our work suggests that decimation of the hippo population over the past decades could have contributed to increased N:Si and P:Si ratios in those lakes.

On longer time scales, the lack of fresh feces and decline in resuspended sediment associated with declining hippo populations could lead to a decrease in river turbidity, creating an opportunity for diatom growth in the river, which could decrease the dissolved Si flux even further. To complicate matters, Si cycling in the savannah ecosystem also would change substantially, as the grassland would transform from a system, where biogenic Si is continuously removed through hippo grazing, to a system with the potential for greater internal recycling of biogenic Si and higher within-soil retention of Si [similar to many other ecosystems around the world (*6*)]. The retention of Si within the nonfluvial part of the ecosystem has the potential to reduce river Si fluxes even further. Thus, the flux of Si to lakes, and the ecosystem services this supports, will likely decline with the loss of hippos and other megafauna, and indeed, modern-day levels may already be a fraction of historical levels before the Pleistocene megafauna extinction (*2*, *36*).

MATERIALS AND METHODS

Field site description

The Mara River (Kenya-Tanzania) has a long-year average discharge of 12.5 $m^3 s^{-1}$ at the Kenya-Tanzania border and contributes about 5% of the volume of water flowing into Lake Victoria (*30*). The Lake Victoria basin is of environmental and biodiversity conservation interest, particularly the Maasai Mara-Serengeti ecosystem. While hippo populations have declined strongly across the African continent due to hunting and terrestrial and aquatic habitat degradation, local densities can still be high. Hippo densities in the Mara River (Kenyan side) reach 36 hippos per km of river, which is the largest single population on the African continent and represents 3% of the total population (*37*).

This study was undertaken in the MMNR in south-western Kenya. Local soils are Versitols, high in clay content and dark in color. This

region has generally bimodal rainy seasons, with short rains from October to December and long rains from March to May (*38*). Ten main field sites were selected on the Mara River based on their accessibility and equal distribution along the river (see map in Fig. 6). The most upstream site 1 lies outside the MMNR and surrounding wildlife conservancies and has almost no hippo activity. Wildlife conservancies begin between sites 1 and 2, and hippo densities rise abruptly (*37*). Site 10 is the most downstream site, just before the Tanzanian border. Three additional sites were selected on the main tributaries of the Mara River. Sites on the Amala and Nyangores lie upstream in urban areas (no wild animals), while the site on the Talek lies between sites 8 and 9 in the MMNR and is inhabited by hippos.

Sampling protocols

All sites were sampled during the dry season (February 2014). River discharge was measured upstream (5.3 $m^3\ s^{-1}$ near site 1) and downstream (5.4 $m^3\ s^{-1}$ near site 10) using depth transducers at rated cross sections. At site 1, stage height was measured every 15 min using a RuggedTROLL 100 pressure transducer that was corrected for atmospheric pressure changes (In-Situ Inc., Fort Collins, CO, USA). At site 10, the stage height was measured every 15 min with a pressure transducer connected to a Eureka Manta2 sonde (Eureka Water Probes, Austin, TX, USA). Rating curves were developed at both sites by measuring discharge using the area-velocity method on multiple occasions in 2011 and 2014 using either a handheld staff gauge or weighted measuring tape for depth and velocimeter for velocity or a HydroSurveyor (SonTek, San Diego, CA, USA). The stage height was converted to discharge using a rating curve developed for each site (*39*). Discharge measurements were averaged over a 10-day period before our sampling campaign.

River water was sampled at all 10 river sites and at all 3 tributary sites. Water quality parameters, including temperature (in°C), pH, EC (in µS cm^{-1}), O_2 (in % and mg $liter^{-1}$), and salinity [in PSU (practical salinity unit)], were monitored with a Eureka Manta2 sonde (Eureka Water Probes, Austin, TX, USA). Total suspended sediment (in mg $liter^{-1}$) was measured by filtering water samples through preweighed filter papers. A plastic syringe was used, and samples were filtered through 0.45-µm nitrocellulose Chromafil syringe filters (A-45/25) into sample bottles and stored cool (4°C) until analysis for dissolved Si concentration (in mg $liter^{-1}$) and dissolved Si δ^{30}Si values.

Suspended matter was sampled at all 10 river sites and at all 3 tributary sites. Water samples of known volume (50 ml) were filtered over nitrocellulose filters with a pore size of 0.45 µm (PORAFIL Membranfilter; Macherey-Nagel, Düren, Germany). Filters were dried for 72 hours at 70°C and analyzed for biogenic Si concentration in the river (in mg $liter^{-1}$ water). To analyze the quality of the biogenic Si (in mg g^{-1} of suspended matter) and δ^{30}Si values, extra samples (~20 liters) were taken at the same locations. Particles could settle for 48 hours after which overlaying water was removed and the remaining slurry was dried at 70°C for 72 hours. Too little material could be sampled from the Nyangores site to analyze biogenic Si (in mg g^{-1}).

Porewater was sampled at river sites 1, 2, 3, 5, 6, 7, and 10 (not at sites 4, 8, and 9 and not at tributary sites). Three standard rhizons (Rhizosphere Research Products, Wageningen, The Netherlands) were inserted 10 cm deep into the sediment (no overlaying water present), and vacuum force was implemented using a standard plastic syringe of 50 ml. The water that accumulated over a period of 15 min was then pooled into one sample for each site, filtered through 0.45-µm nitrocellulose Chromafil syringe filters (A-45/25) into sample bottles, and stored cool (4°C) until analysis for dissolved Si concentration (mg $liter^{-1}$) and dissolved Si δ^{30}Si values (no analysis for site 5).

Sediment was sampled at all 10 river sites. Cores (20 cm long and 28 mm in diameter) were sampled per site using a hammer auger with a removable plastic lining (Eijkelkamp 04.15.SA Foil sampler; Giesbeek, The Netherlands). Immediately after sampling, each core was subsectioned into six slices, with 2-cm intervals each in the top 10 cm of the core and the sixth slice containing the rest of the core. All slices were packed in vacuum plastic bags and stored cool (4°C) on return to the laboratory. Samples were dried for 72 hours at 70°C and homogenized by manual grinding before analysis. Biogenic Si concentration (in mg g^{-1}) was determined in slices 1 (0 to −2 cm), 3 (−4 to −6 cm), and 5 (−8 to −10 cm). Biogenic Si δ^{30}Si values were determined on all slices.

Grass and hippo feces were sampled at all nine river sites within the conservancy, and grass was sampled at site 1 and tributaries Amala and Nyangores (not at Talek). Monospecific stands of the dominating grass species were selected on hippo grazing lawns flanking the different sites. These lawns are areas relatively close to the river that are frequently grazed by hippos (*40*). One sample per site was cut in a quadrant of 60 cm × 60 cm. Hippo feces (if present) were sampled as close as possible to the grass plot. An ad hoc grab sample was taken from feces that visibly appeared to be fresh (still moist and uncontaminated with dust). Grass and fecal samples were dried for 72 hours at 70°C and mechanically ground before analysis for biogenic Si concentration (in mg g^{-1}) and biogenic Si δ^{30}Si values.

One hippo pool was selected on the Mara River between sites 7 and 8 (see map in Fig. 6). The hippo pool is a local aggregation of hippos that remain in their territory. Automatic water samplers (3700C Compact Portable Sampler; Teledyne ISCO, Lincoln, NE, USA) were placed upstream and downstream of this hippo pool and programmed to collect one sample every other hour for a 24-hour period (18 February 2014 11:00 a.m. to 19 February 2014 11:00 a.m.). Samples stayed cool in the samplers during this period, and weather and river hydraulic conditions remained stable. The distance between both samplers was 250 m measured along the river, and a maximum of 80 hippos were counted. Subsamples of all water samples were filtered through 0.45-µm nitrocellulose Chromafil syringe filters (A-45/25) into sample bottles and stored cool (4°C) until analysis for dissolved Si concentration (mg $liter^{-1}$). Subsamples of 50 ml were filtered over nitrocellulose filters with a pore size of 0.45 µm (PORAFIL Membranfilter; Macherey-Nagel, Düren, Germany). Filters were dried for 72 hours at 70°C and analyzed for biogenic Si concentration (in mg $liter^{-1}$).

Last, in the savannah grassland, three random plots were sampled in February 2014 and supplemented by three extra plots in August 2016 (see map in Fig. 6). These plots were roughly located near sites 2, 5, 6, 8, 9, and 10 but were not under direct influence of the river (a distance of >1 km perpendicular to the river). Soil cores of the Versitol that dominates the MMNR savannah were sampled in a similar way as the sediment cores. Immediately after sampling, each core was subsectioned into two slices of 5 and 10 cm (2014 samples) or into one slice of the top 5 cm (2016 samples), packed in vacuum plastic bags and stored cool (4°C) until return to the laboratory. Samples were dried for 72 hours at 70°C and homogenized by manual grinding before analysis. Biogenic Si concentration (in mg g^{-1}) was determined on all slices. Biogenic Si δ^{30}Si values were determined for the top slices of samples near sites 9 and 10.

Chemical analysis protocols

All Si concentrations are reported as the mass of elemental Si and not the mass of SiO_2. All water samples (from river water, porewater, and the hippo pool) were analyzed for dissolved Si concentration on an Inductive Coupled Plasma Atomic Emission Spectrophotometer (ICP-AES, Thermo Fisher Scientific, ICAP 6000 Series).

Grass, feces, and suspended matter sampled on filters were analyzed for biogenic Si concentration in a classical manner. A sample of 25 mg of dry matter (for grass and feces) or the entire filter (for suspended matter) was incubated in 25 ml of 0.5 M NaOH at 80°C for 5 hours. The extracted and dissolved Si was analyzed colorimetrically on a segmented flow analyzer (San++; Skalar, Breda, The Netherlands), after it had passed a dialyzer module separating the analyte from interfering substances (e.g., the yellow color from the nitrocellulose filters). The extraction in 0.1 M NaOH at 80°C has been well established and tested; it is capable of fully dissolving the biogenic Si from plant phytoliths at the solid/solution ratios and extraction time we applied (*41*).

Sediment, soil, and suspended matter sampled by settlement are usually a mixture of biogenic Si and mineral Si, and a classic analysis will not distinguish between different reactive fractions. Therefore, the samples were extracted using a novel alkaline continuous extraction in NaOH, according to the method from (*42*). Si and Al concentrations are measured continuously, and the two dissolution curves are fitted together in a first-order equation (Eqs. 1 and 2)

$$\mathrm{Si}_t = \left(\sum_{i=1}^{n} \mathrm{AlkExSi}_i \times \left(1 - e^{-k_i \times t}\right)\right) + b \times t \quad (1)$$

$$\mathrm{Al}_t = \left(\sum_{i=1}^{n} \frac{\mathrm{AlkExSi}_i}{\mathrm{Si/Al_i}} \times \left(1 - e^{-k_i \times t}\right)\right) + \frac{b \times t}{\mathrm{Si/Al_{min}}} \quad (2)$$

This method distinguishes between fractions dissolving linearly (poor reactive silica) and those exhibiting a nonlinear behavior (highly reactive silica). Linear fractions are characterized by parameters *b* (slope of the linear dissolution) and Si/Al (ratio of Si and Al in that fraction); nonlinear fractions are characterized by the amount of AlkExSi (alkaline extractable silica; in mg g^{-1} of sample), *k* [reactivity of the fraction in NaOH (in mg g^{-1} min^{-1})], and Si/Al (ratio of Si and Al in that fraction). In contrast to the more traditional time course extraction method used for soils (extractions at hours 3, 4, and 5 in a weak base), which also distinguishes between biogenic and mineral silicates based on regression slopes, this new method also allows distinguishing between different reactive silica fractions (with *k* values > 0.1) according to their origin based on the Si/Al ratio determined by the model: true biogenic Si (Si/Al ratio of ≥4), Si belonging to clay minerals (Si/Al ratio between 1 and 4), and Si absorbed by oxides (Si/Al ratio of ≤1). More details about the continuous alkaline extraction of Si and Al method can be found in (*42*). We present data of the true biogenic Si (noted as AlkExSi_biogenic Si) and the sum of the other reactive fractions (noted as AlkExSi_non_biogenic Si) in table S2. Nonreactive fractions are not shown.

Batch dissolution experiment protocol

To mimic in situ reactivity of Si after digestion, Si dissolution from six different samples was monitored over different time intervals in rain water [methodology after (*18*)]. The samples were (i) fresh hippo feces (<24 hours old, still wet when sampled), (ii) dried hippo feces (desiccated and visual confirmation of its presence days before sampling), (iii) old hippo feces (dried out and visual conformation of its presence weeks before sampling), (iv) grass (freshly cut in 1-cm pieces), (v) sediment (dried and homogenized), and (vi) Versitol from the savannah grassland (dried and homogenized). All samples came from or near site 10. Fresh material (3 g) was put in 200-ml plastic boxes and spread out evenly over the bottom surface (ca. 40 cm^2). In total, 341 boxes were prepared and sampled destructively over time: five replicates per different sample per time interval and one blank per time interval. At the start of each experiment, all boxes were filled with 30 ml of air-captured rain water (pH 7.18, EC of 23.5 μS cm^{-1}, and a natural background dissolved Si concentration of 0.17 mg $liter^{-1}$, which was corrected for in the calculations). Dissolution experiments were carried out for 24 hours in a dark incubator at 20°C, and subsamples were taken at 11 time intervals (2, 5, 10, and 30 min and 1, 2, 5, 10, 15, 18, and 24 hours). At each time interval, 10 ml of solution was sampled from a box and filtered through 0.45-μm nitrocellulose Chromafil syringe filters (A-45/25) and analyzed for dissolved Si using ICP-AES. The sampled box was not further used. Results are plotted relative to the respective reactive Si concentration (i.e., biogenic Si for grass and feces and AlkExSi for sediment and soil). A subsample of the "old feces" was also analyzed for its isotopic δ^{30}Si value and compared to the average value of fresh feces sampled and analyzed before.

Diatom and phytolith fixation protocol

The presence or absence of biogenic Si particles (diatom frustules, chrysophyte stomatocysts, and phytoliths) was determined in suspended matter samples and uppermost 2-cm sediment samples of sites 1, 5, and 10. In addition, feces and grass samples were prepared to check their phytolith contents. Samples were prepared for light microscopy (LM) following the method described in (*43*). Small parts of the sample were cleaned by adding 37% H_2O_2 and heating to 80°C for about 1 hour. The reaction was completed by addition of $KMnO_4$. Following digestion and centrifugation (three times for 10 min at 3700*g*), the cleaned material was diluted with distilled water to avoid excessive concentrations of diatoms and phytoliths on the slides. Cleaned diatom material was mounted in Naphrax. The slides were analyzed using an Olympus BX53 microscope, equipped with Differential Interference Contrast (Nomarski) and the Olympus UC30 Imaging System. The variation in biogenic Si particles was visualized (fig. S1) and was counted on random transects at 400× magnification, and the relative abundance of each group (diatoms, chrysophytes, and phytoliths) was determined.

Si isotope analysis protocol

A selection ($n = 71$) of the samples was analyzed for δ^{30}Si: river water samples of all 10 sites and the three tributary sites; porewater samples of sites 1, 2, 3, 6, 7, and 10; suspended matter samples of all 10 sites; grass and fecal samples of sites 3, 5, 8, and 10; sediment of sites 1, 3, 5, 8, and 10 (all slices per core were analyzed and averaged per site); and finally, all uppermost slices of two Versitol samples from the savannah grassland. Sample preparation followed a standard two-step purification procedure (*24*) in which the Si was first leached or concentrated from the sample and then chromatographically purified before introduction to a MC-ICP Mass Spectrometer. See the Supplementary Materials for a detailed description of this Si isotope analysis protocol and of the Si isotope mass balance model.

SUPPLEMENTARY MATERIALS

Supplementary material for this article is available at http://advances.sciencemag.org/cgi/content/full/5/5/eaav0395/DC1

Supplementary Materials and Methods

Fig. S1. Biogenic Si particles observed in suspended matter and sediment samples.

Fig. S2. Results from mass balance calculations.
Fig. S3. Results from the rain water batch dissolution experiment.
Table S1. Abiotic data and results of chemical Si analyses.
Table S2. Summary of Si isotope analyses presented in this paper.
References (*44*–*60*)

REFERENCES AND NOTES

1. S. Bauer, B. J. Hoye, Migratory animals couple biodiversity and ecosystem functioning worldwide. *Science* **344**, 1242552 (2014).
2. C. E. Doughty, J. Roman, S. Faurby, A. Wolf, A. Haque, E. S. Bakker, Y. Malhi, J. B. J. Dunning Jr., J.-C. Svenning, Global nutrient transport in a world of giants. *Proc. Natl. Acad. Sci. U.S.A.* **113**, 868–873 (2016).
3. E. S. Bakker, J. F. Pages, R. Arthur, T. Alcoverro, Assessing the role of large herbivores in the structuring and functioning of freshwater and marine angiosperm ecosystems. *Ecography* **39**, 162–179 (2016).
4. O. J. Schmitz, P. A. Raymond, J. A. Estes, W. A. Kurz, G. W. Holtgrieve, M. E. Ritchie, D. E. Schindler, A. C. Spivak, R. W. Wilson, M. A. Bradford, V. Christensen, L. Deegan, V. Smetacek, M. J. Vanni, C. C. Wilmers, Animating the carbon cycle. *Ecosystems* **17**, 344–359 (2014).
5. E. Struyf, D. J. Conley, Emerging understanding of the ecosystem silica filter. *Biogeochemistry* **107**, 9–18 (2012).
6. J. Schoelynck, F. Müller, F. Vandevenne, K. Bal, L. Barao, A. Smis, W. Opdekamp, P. Meire, E. Struyf, Silicon-vegetation interaction in multiple ecosystems: A review. *J. Veg. Sci.* **25**, 301–313 (2014).
7. J. C. Carey, R. W. Fulweiler, The terrestrial silica pump. *PLOS ONE* **7**, e52932 (2012).
8. E. V. Armbrust, The life of diatoms in the world's oceans. *Nature* **459**, 185–192 (2009).
9. V. Martin-Jézéquel, M. Hildebrand, M. A. Brzezinski, Silicon metabolism in diatoms: Implications for growth. *J. Phycol.* **36**, 821–840 (2000).
10. H. E. Cockerton, F. A. Street-Perrott, P. A. Barker, M. J. Leng, H. J. Sloane, K. J. Ficken, Orbital forcing of glacial/interglacial variations in chemical weathering and silicon cycling within the upper White Nile basin, East Africa: Stable-isotope and biomarker evidence from Lakes Victoria and Edward. *Quat. Sci. Rev.* **130**, 57–71 (2015).
11. H. A. Bootsma, R. E. Hecky, T. C. Johnson, H. J. Kling, J. Mwita, Inputs, outputs, and internal cycling of silica in a large, tropical lake. *J. Great Lakes Res.* **29**, 121–138 (2003).
12. P. Kilham, Hypothesis concerning silica and freshwater planktonic diatoms. *Limnol. Oceanogr.* **16**, 10–18 (1971).
13. D. Verschuren, T. C. Johnson, H. J. Kling, D. N. Edgington, P. R. Leavitt, E. T. Brown, M. R. Talbot, R. E. Hecky, History and timing of human impact on Lake Victoria, East Africa. *Proc. Biol. Sci.* **269**, 289–294 (2002).
14. A. L. Subalusky, C. L. Dutton, E. J. Rosi-Marshall, D. M. Post, The hippopotamus conveyor belt: Vectors of carbon and nutrients from terrestrial grasslands to aquatic systems in sub-Saharan Africa. *Freshw. Biol.* **60**, 512–525 (2015).
15. F. I. Vandevenne, E. Struyf, W. Clymans, P. Meire, Agricultural silica harvest: Have humans created a new and important loop in the global silica cycle? *Front. Ecol. Environ.* **10**, 243–248 (2012).
16. H. J. Hughes, F. Sondag, C. Cocquyt, A. Laraque, A. Pandi, L. André, D. Cardinal, Effect of seasonal biogenic silica variations on dissolved silicon fluxes and isotopic signatures in the Congo River. *Limnol. Oceanogr.* **56**, 551–561 (2011).
17. L. Cary, A. Alexandre, J.-D. Meunier, J.-L. Boeglin, J.-J. Braun, Contribution of phytoliths to the suspended load of biogenic silica in the Nyong basin rivers (Cameroon). *Biogeochemistry* **74**, 101–114 (2005).
18. F. Vandevenne, L. Barão, J. Schoelynck, A. Smis, N. Ryken, S. Van Damme, P. Meire, E. Struyf, Grazers: Bio-catalysts of terrestrial silica cycling. *Proc. Roy. Sci. B* **280**, 20132083 (2013).
19. C. Dutton, S. C. Anisfeld, H. Ernstberger, A novel sediment fingerprinting method using filtration: Application to the Mara River, East Africa. *J. Soils Sediments* **13**, 1708–1723 (2013).
20. P. J. Frings, W. Clymans, G. Fontorbe, C. L. De La Rocha, D. J. Conley, The continental Si cycle and its impact on the ocean Si isotope budget. *Chem. Geol.* **425**, 12–36 (2016).
21. S. Opfergelt, D. Cardinal, C. Henriet, X. Draye, L. André, B. Delvaux, Silicon isotopic fractionation by banana (*Musa* spp.) grown in a continuous nutrient flow device. *Plant Soil* **285**, 333–345 (2006).
22. L. H. P. Jones, K. A. Handreck, Silica in soils, plants, and animals. *Adv. Agron.* **19**, 107–149 (1967).
23. M. S. Demarest, M. A. Brzezinski, C. P. Beucher, Fractionation of silicon isotopes during biogenic silica dissolution. *Geochim. Cosmochim. Acta* **73**, 5572–5583 (2009).
24. P. J. Frings, C. De La Rocha, E. Struyf, D. van Pelt, J. Schoelynck, M. M. Hudson, M. J. Gondwe, P. Wolski, K. Mosimane, W. Gray, J. Schaller, D. J. Conley, Tracing silicon cycling in the Okavango Delta, a sub-tropical flood-pulse wetland using silicon isotopes. *Geochim. Cosmochim. Acta* **142**, 132–148 (2014).
25. M. Oelze, F. von Blanckenburg, D. Hoellen, M. Dietzel, J. Bouchez, Si stable isotope fractionation during adsorption and the competition between kinetic and equilibrium isotope fractionation: Implications for weathering systems. *Chem. Geol.* **380**, 161–171 (2014).
26. A. L. Subalusky, C. L. Dutton, S. C. Anisfeld, L. Njoroge, E. J. Rosi, D. M. Post, Organic matter and nutrient inputs from large wildlife influence ecosystem function in the Mara River, Africa. *Ecology* **99**, 2558–2574 (2018).
27. E. Struyf, K. Mosimane, D. Van Pelt, M. Murray-Hudson, P. Meire, P. Frings, P. Wolski, J. Schaller, M. J. Gondwe, J. Schoelynck, D. J. Conley, The role of vegetation in the Okavango Delta silica sink. *Wetlands* **35**, 171–181 (2015).
28. C. E. Doughty, Herbivores increase the global availability of nutrients over millions of years. *Nat. Ecol. Evol.* **1**, 1820–1827 (2017).
29. F. Müller, E. Struyf, J. Hartmann, A. Weiss, K. Jensen, Impact of grazing management on silica export dynamics of Wadden Sea saltmarshes. *Estuar. Coast. Shelf Sci.* **127**, 1–11 (2013).
30. F. O. Masese, M. E. McClain, Trophic resources and emergent food web attributes in rivers of the Lake Victoria Basin: A review with reference to anthropogenic influences. *Ecohydrology* **5**, 685–707 (2012).
31. R. Lewison, J. Pluháček, *Hippopotamus amphibius*. The IUCN Red List of Threatened Species 2017: e.T10103A18567364; http://dx.doi.org/10.2305/IUCN.UK.2017-2.RLTS.T10103A18567364.en.
32. D. Verschuren, D. N. Edgington, H. J. Kling, T. C. Johnson, Silica depletion in Lake Victoria: Sedimentary signals at offshore stations. *J. Great Lakes Res.* **24**, 118–130 (1998).
33. C. Stager, R. E. Hecky, D. Grzesik, B. F. Cumming, H. Kling, Diatom evidence for the timing and causes of eutrophication in Lake Victoria, East Africa. *Hydrobiologia* **636**, 463–478 (2009).
34. D. M. Anderson, P. M. Gilbert, J. M. Burkholder, Harmful algal blooms and eutrophication nutrient sources, composition and consequences. *Estuaries* **25**, 704–726 (2002).
35. J. E. Tierney, M. T. Mayes, N. Meyer, C. Johnson, P. W. Swarzenski, A. S. Cohen, J. M. Russell, Late-twentieth-century warming in Lake Tanganyika unprecedented since AD 500. *Nat. Geosci.* **3**, 422–425 (2010).
36. C. E. Doughty, A. Wolf, Y. Malhi, The legacy of the Pleistocene megafauna extinctions on nutrient availability in Amazonia. *Nat. Geosci.* **6**, 761–764 (2013).
37. E. M. Kanga, J. O. Ogutu, H. Olff, P. Santema, Population trend and distribution of the Vulnerable common hippopotamus *Hippopotamus amphibius* in the Mara Region of Kenya. *Oryx* **45**, 20–27 (2011).
38. M. E. McClain, A. L. Subalusky, E. P. Anderson, S. B. Dessu, A. M. Melesse, P. M. Ndomba, J. O. D. Mtamba, R. A. Tamatamah, C. Mligo, Comparing flow regime, channel hydraulics, and biological communities to infer flow-ecology relationships in the Mara River of Kenya and Tanzania. *Hydrol. Sci. J.* **59**, 801–819 (2014).
39. C. L. Dutton, A. L. Subalusky, S. C. Anisfeld, L. Njoroge, E. J. Rosi, D. M. Post, The influence of a semi-arid sub-catchment on suspended sediments in the Mara River, Kenya. *PLOS ONE* **13**, e0192828 (2018).
40. C. R. Field, A study of the feeding habits of the hippopotamus (*Hippopotamus amphibius* Linn.) in the Queen Elizabeth National Park, Uganda, with some management implications. *Afr. Zool.* **5**, 71–86 (1970).
41. D. J. DeMaster, The supply and accumulation of silica in the marine-environment. *Geochim. Cosmochim. Acta* **45**, 1715–1732 (1981).
42. L. Barão, W. Clymans, F. Vandevenne, P. Meire, D. J. Conley, E. Struyf, Pedogenic and biogenic alkaline-extracted silicon distributions along a temperate land-use gradient. *Eur. J. Soil Sci.* **65**, 693–705 (2014).
43. A. van der Werf, A new method of concentrating and cleaning diatoms and other organisms. *Verh. Int. Ver. Limnol.* **12**, 276–277 (1955).
44. C. L. De La Rocha, M. A. Brzezinski, M. J. DeNiro, Purification, recovery, and laser-driven fluorination of silicon from dissolved and particulate silica for the measurement of natural stable isotope abundances. *Anal. Chem.* **68**, 3746–3750 (1996).
45. E. Engstrom, I. Rodushkin, D. C. Baxter, B. Ohlander, Chromatographic purification for the determination of dissolved silicon isotopic compositions in natural waters by high-resolution multicollector inductively coupled plasma mass spectrometry. *Anal. Chem.* **78**, 250–257 (2006).
46. R. B. Georg, B. C. Reynolds, M. Frank, A. N. Halliday, New sample preparation techniques for the determination of Si isotopic compositions using MC-ICPMS. *Chem. Geol.* **235**, 95–104 (2006).
47. B. C. Reynolds, J. Aggarwal, L. Andre, D. Baxter, C. Beucher, M. A. Brzezinski, E. Engstrom, R. B. Georg, M. Land, M. J. Leng, S. Opfergelt, I. Rodushkin, H. J. Sloane, S. H. J. M. van den Boorn, P. Z. Vroon, D. Cardinal, An inter-laboratory comparison of Si isotope reference materials. *J. Anal. At. Spectrom.* **22**, 561–568 (2007).
48. D. Cardinal, L. Y. Alleman, J. de Jong, K. Ziegler, L. Andre, Isotopic composition of silicon measured by multicollector plasma source mass spectrometry in dry plasma mode. *J. Anal. At. Spectrom.* **18**, 213–218 (2003).
49. M. Oelze, F. von Blanckenburg, J. Bouchez, D. Hoellen, M. Dietzel, The effect of Al on Si isotope fractionation investigated by silica precipitation experiments. *Chem. Geol.* **397**, 94–105 (2015).
50. K. Ziegler, O. A. Chadwick, A. F. White, M. A. Brzezinski, δ^{30}Si systematics in a granitic saprolite, Puerto Rico. *Geology* **33**, 817–820 (2005).
51. S. Opfergelt, R. B. Georg, B. Delvaux, Y.-M. Cabidoche, K. W. Burtona, A. N. Hallidaya, Silicon isotopes and the tracing of desilication in volcanic soil weathering sequences, Guadeloupe. *Chem. Geol.* **326–327**, 113–122 (2012).

52. S. Opfergelt, P. Delmelle, Silicon isotopes and continental weathering processes: Assessing controls on Si transfer to the ocean. *C. R. Geosci.* **344**, 723–738 (2012).
53. T. P. Ding, S. H. Tian, L. Sun, L. H. Wu, J. X. Zhou, Z. Y. Chen, Silicon isotope fractionation between rice plants and nutrient solution and its significance to the study of the silicon cycle. *Geochim. Cosmochim. Acta* **72**, 5600–5615 (2008).
54. T. P. Ding, J. X. Zhou, D. F. Wan, Z. Y. Chen, C. Y. Wang, F. Zhang, Silicon isotope fractionation in bamboo and its significance to the biogeochemical cycle of silicon. *Geochim. Cosmochim. Acta* **72**, 1381–1395 (2008).
55. L. Y. Alleman, D. Cardinal, C. Cocquyt, P.-D. Plisnier, J.-P. Descy, I. Kimirei, D. Sinyinza, L. André, Silicon isotopic fractionation in Lake Tanganyika and its main tributaries. *J. Great Lakes Res.* **31**, 509–519 (2005).
56. K. Ziegler, O. A. Chadwick, M. A. Brzezinski, E. F. Kelly, Natural variations of delta Si-30 ratios during progressive basalt weathering, Hawaiian Islands. *Geochim. Cosmochim. Acta* **69**, 4597–4610 (2005).
57. F. Fraysse, O. S. Pokrovsky, J. Schott, J.-D. Meunier, Surface properties, solubility and dissolution kinetics of bamboo phytoliths. *Geochim. Cosmochim. Acta* **70**, 1939–1951 (2006).
58. D. Rickert, M. Schlüter, K. Wallmann, Dissolution kinetics of biogenic silica from the water column to the sediments. *Geochim. Cosmochim. Acta* **66**, 439–455 (2002).
59. P. Van Cappellen, L. Qiu, Biogenic silica dissolution in sediments of the Southern Ocean .1. Solubility. *Deep Sea Res. Part 2 Top. Stud. Oceanogr.* **44**, 1109–1128 (1997).
60. A. Kamatani, N. Ejiri, P. Treguer, The dissolution kinetics of diatom ooze from the Antarctic area. *Deep Sea Res. A Oceanogr. Res. Pap.* **35**, 1195–1203 (1988).

Acknowledgments: We would like to thank C. Cocquyt for her valuable comments that improved this manuscript. **Funding:** J.S. is a postdoctoral fellow of FWO (project no. 12H8616N) and had an FWO travel grant (K203714N). D.U.-B. thanks BELSPO for PhD funding in the project SOGLO (SOil System under GLObal change). Research in the Mara River was conducted in affiliation with the National Museums of Kenya under research permit number NCST/RCD/12B/012/36 from the Kenya National Commission for Science, Technology and Innovation and was funded by U.S. National Science Foundation grants to D.M.P. (NSF DEB 1354053 and DEB 1753727) and E.J.R. (NSF DEB 1354062). This is Vegacenter publication #015, published with support from the Belgian University Foundation. **Author contributions:** J.S. is the principal investigator of the study, was involved in all parts of the research, and wrote the manuscript. A.L.S., E.S., C.L.D., D.U.-B., and P.F. equally contributed to field and laboratory work, wrote substantial parts of the text, and proofread the entire manuscript. B.V.d.V. was in charge of LM to visualize phytoliths and counting Si particles, wrote significant parts of the text, and proofread the entire manuscript. D.M.P., E.J.R., and P.M. are promotors of the study, financed and facilitated a significant part of the work, and proofread the entire manuscript. **Competing interests:** The authors declare that they have no competing interests. **Data and materials availability:** All data needed to evaluate the conclusions in the paper are present in the paper and/or the Supplementary Materials. Additional data related to this paper may be requested from the authors.

Submitted 8 August 2018
Accepted 21 March 2019
Published 1 May 2019
10.1126/sciadv.aav0395

Citation: J. Schoelynck, A. L. Subalusky, E. Struyf, C. L. Dutton, D. Unzué-Belmonte, B. Van de Vijver, D. M. Post, E. J. Rosi, P. Meire, P. Frings, Hippos (*Hippopotamus amphibius*): The animal silicon pump. *Sci. Adv.* **5**, eaav0395 (2019).